

^{199}Hg Knight shift and spin-lattice relaxation in $\text{HgBa}_2\text{CuO}_{4+\delta}$

B. J. Suh

Ames Laboratory and Department of Physics and Astronomy, Iowa State University, Ames, Iowa 50011

F. Borsa

*Ames Laboratory and Department of Physics and Astronomy, Iowa State University, Ames, Iowa 50011
and Dipartimento di Fisica "A. Volta," Universita di Pavia, 27100 Pavia, Italy*

Ming Xu and D. R. Torgeson

Ames Laboratory and Department of Physics and Astronomy, Iowa State University, Ames, Iowa 50011

W. J. Zhu, Y. Z. Huang, and Z. X. Zhao

*National Laboratory for Superconductivity, Institute of Physics, Academia Sinica, Beijing 100080, China
(Received 21 March 1994)*

^{199}Hg NMR spectra and T_1^{-1} are reported for two samples of $\text{HgBa}_2\text{CuO}_{4+\delta}$ with superconducting transitions at $T_c=95$ K and $T_c=80$ K, respectively. The spectra are characteristic powder patterns with large anisotropic shifts: $3K_{\text{ax}}=-0.43\%$ and -0.52% , respectively, for the two samples at room temperature with negligible temperature dependence below T_c . The isotropic Knight shifts were of order $K_{\text{iso}}=+0.11\%$ with respect to a $\text{Hg}(\text{NO}_3)_2$ aqueous solution. The relaxation rate is Korringa-like above T_c while below T_c the relaxation rate drops down exponentially without enhancement near T_c .

The recently discovered high- T_c superconductor $\text{HgBa}_2\text{CuO}_{4+\delta}$ is of particular interest since it has the highest critical temperature ($T_c=95$ K) among the single CuO_2 layered compounds.¹ One attractive feature of the system is its relatively simple structure.^{2,3} There is only one kind of Cu site in the usual square planar coordination with four oxygen atoms and the copper oxide planes are linked by the O-Hg-O chains which involve the apical oxygens [denoted O(2)]. The addition of oxygen to the interstitial sites in the planes of mercury atoms appears to be the doping mechanism responsible for the conducting and the superconducting properties of the system.² An additional point of interest concerns the magnetic properties since the irreversibility line is intermediate between the characteristic strongly pinned flux lines in Y-Ba-Cu-O compounds and the weakly pinned Bi-based and Tl-based compounds.⁴

The ^{199}Hg nucleus ($I=\frac{1}{2}$) is a promising probe for a NMR study of the electronic properties in view of the lack of quadrupole interaction, the large atomic hyperfine coupling constant, and its location in the crystal lattice.

In this paper we report a ^{199}Hg NMR study in two powder samples of single-phase $\text{HgBa}_2\text{CuO}_{4+\delta}$ with $T_c=95$ K and $T_c=80$ K, respectively. The shift of the NMR line is found to be highly anisotropic reflecting the linear configuration of the Hg-O(2) bonds in the dumbbell shape. The nuclear spin-lattice relaxation rate is found to be driven by the coupling with the Fermi liquid of the electronic carriers and it gives information about the opening of the superconducting energy gap.

The samples were prepared by heating stoichiometric amounts of oxides HgO, BaO, and CuO sealed in a silica tube evacuated to 10^{-2} Torr. The heating cycle was: heating a rate of $200^\circ\text{C}/\text{h}$ up to 680 to 750°C , holding for 0.5 – 10 h, and then cooling down slowly to room temperature. The pel-

lets were annealed at 260°C in an oxygen atmosphere for 6 h (sample A). Part of the sample A was further annealed in flowing argon at 450°C for 24 h to reduce the oxygen content and consequently T_c (from $T_c=95$ K to $T_c=80$ K). Two samples of $\text{HgBa}_2\text{CuO}_{4+\delta_A, \delta_B}$ ($\delta_A > \delta_B$) were finally prepared in powder form for the NMR measurements: sample A ($T_c=95$ K) and sample B ($T_c=80$ K). Both samples show the same x-ray powder-diffraction pattern. The x-ray spectrum for sample A is shown in Fig. 1. All peaks can be indexed by the tetragonal $\text{HgBa}_2\text{CuO}_{4+\delta}$ structure^{2,4} with lattice parameters: $a=3.87$ Å and $c=9.49$ Å. No observable lines of spurious phases are present.

The zero-field-cooled magnetization curves are shown in Fig. 2. The Meissner fraction is estimated to be about 60% for sample A and 30% for sample B, which are quite reasonable values for powder samples. Sample powders were assumed for simplicity to be spherical in shape so a demagnetization factor of $\frac{1}{3}$ was used.

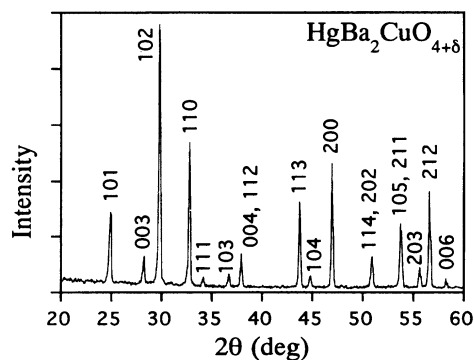


FIG. 1. X-ray powder-diffraction data for the powder $\text{HgBa}_2\text{CuO}_{4+\delta}$ sample A.

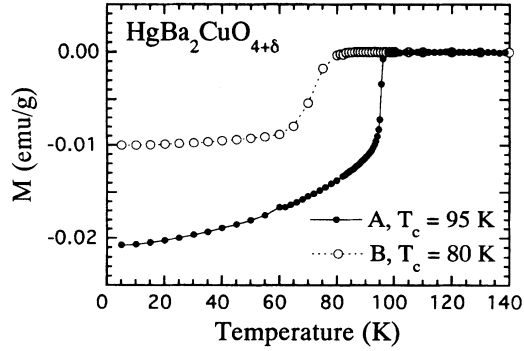


FIG. 2. Zero-field-cooled magnetization vs temperature. The two $\text{HgBa}_2\text{CuO}_{4+\delta}$ samples, A and B, differ by the excess oxygen content δ , $\delta_A > \delta_B$.

^{199}Hg NMR measurements were performed with a phase coherent pulse Fourier transform (FT) spectrometer at 8.2 T with a few measurements performed also at 4.7 T. A broad ^{199}Hg spectrum was obtained by plotting the intensity of the echo signal following a $(\pi/2)_x - \tau - (\pi)_y$ sequence as a function of a series of discrete spectrometer frequencies. rf pulses with long pulse length and small amplitude were used to reduce experimental broadening effects. The typical $\pi/2$ pulse length was 20 μsec corresponding to an rf magnetic field strength of 16 G. The nuclear spin-lattice relaxation rate measurements were performed by monitoring the echo signal for a variable time after the end of a saturating pulse train of several $\pi/2$ pulses. The recovery of the magnetization was found to be exponential at all temperatures.

The ^{199}Hg NMR spectra at several representative temperatures are shown in Fig. 3 for both samples A ($T_c = 95$ K) and B ($T_c = 80$ K). In the normal state ($T > T_c$) the spectra were textbook examples of a powder pattern in the presence of axially symmetric anisotropic shift tensor⁵ and no measurable temperature dependence was observed. For $T < T_c$ the center of gravity of the spectrum shifts slightly to lower frequency and the line width of each component of the powder pattern increases. The shift to lower frequency is due in part to demagnetization effects and in part to the suppression of the isotropic Knight-shift component by the opening of the superconducting energy gap. The separation of the two effects is impossible in a randomly oriented powder sample. The broadening of the NMR line below T_c is associated with vortex lattice. The situation is similar to the one found for $^{203,205}\text{Tl}$ NMR in $\text{Tl}_2\text{Ba}_2\text{Ca}_2\text{Cu}_3\text{O}_{10+\delta}$.⁶ The values of the isotropic component of the shift $K_{\text{iso}} = (K_{\parallel} + 2K_{\perp})/3$ and for the axial component $3K_{\text{ax}} = K_{\parallel} - K_{\perp}$ are reported in Table I

TABLE I. ^{199}Hg Knight shifts K_{iso} and $3K_{\text{ax}}$ values for two temperatures for samples A and B. ^{199}Hg T_1T values in the normal state ($T > T_c$) for samples A and B.

$\text{HgBa}_2\text{CuO}_{4+\delta}$	T (K)	K_{iso} (%)	$3K_{\text{ax}}$ (%)	T_1T (sec K)
Sample A ($T_c = 95$ K)	294	+0.11	-0.43	10.5
	42	+0.08	-0.41	
Sample B ($T_c = 80$ K)	294	+0.10	-0.52	12.3
	41	+0.08	-0.49	

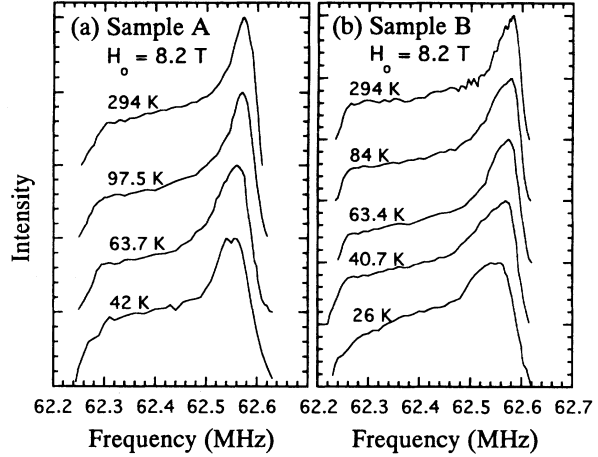


FIG. 3. Representative ^{199}Hg NMR spectra at $H_0 = 8.2$ T for samples A and B. The spectra were obtained point by point by plotting the echo intensity vs a series of spectrometer frequencies. Each spectrum contains about 100 points which have been interpolated.

for two temperatures. Here K_{\parallel} and K_{\perp} refer to the shift for grains in the powder having the c axis parallel and perpendicular to the applied magnetic field, respectively, and were measured with respect to the ^{199}Hg resonance in an aqueous solution of $\text{Hg}(\text{NO}_3)_2$.

We discuss first the axial component of the shift whose value does not depend upon the choice of the ^{199}Hg NMR reference sample or gyromagnetic ratio. The contribution to the shift anisotropy from the dipolar field at the ^{199}Hg site, due to the two nearest-neighbor Cu electron spins above and below the Hg nucleus along the c axis, can be calculated from the expression

$$3K_{\text{ax}} = K_{\parallel} - K_{\perp} = -\frac{2}{r^3} \frac{(2\mu_{\parallel} + \mu_{\perp})}{H_0}, \quad (1)$$

where $\mu_{\parallel, \perp}$ are the paramagnetic moments of the Cu ion induced by the applied field H_0 . Assuming an isotropic susceptibility per atom $\chi = \mu/H_0 = 4 \times 10^{-28}$ which was measured in CuO_2 -based high- T_c systems⁷ and from the known Hg-Cu distance,^{2,3} one has $3K_{\text{ax}} \approx -10^{-3}\%$, which is negligible compared to the experimental value in Table I. Since $3K_{\text{ax}}$ does not change appreciably below T_c , we can tentatively conclude the large observed anisotropy originates mostly from the orbital currents induced by the field H_0 in the linear dumbbell configuration of the Hg-O(2) bond. This large chemical shift anisotropy can include, in principle, both diamagnetic terms and paramagnetic terms. Using Ramsey's expression⁸ the calculated shift can yield information about the Hg-O(2) bonding wave functions. The increase of $3K_{\text{ax}}$ in sample B is in qualitative agreement with the decrease of the Hg-O(2) distance when some of the excess interstitial oxygen are removed.² If the electronic currents set up by the magnetic field were localized around the oxygen atoms one could use a crude dipolar approximation to estimate the effective orbital moment μ needed to explain the anisotropic shift. By using, in Eq. (1), $r = 1.977$ Å [Hg-O(2) distance] and $H_0 = 8.2$ T one finds $\mu \approx 0.04\mu_B$ (μ_B is a Bohr mag-

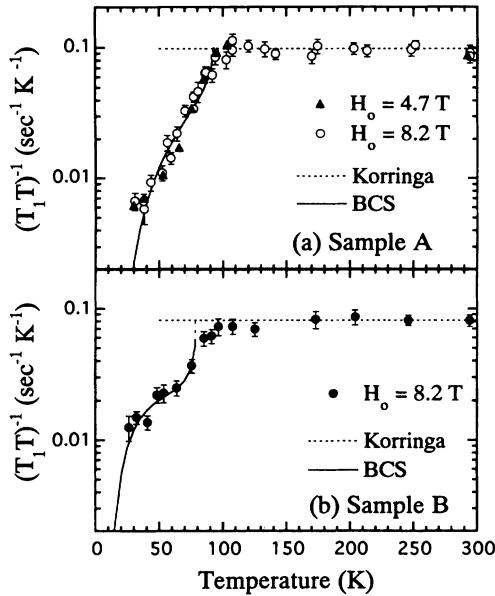


FIG. 4. $(T_1T)^{-1}$ vs temperature of ^{199}Hg in $\text{HgBa}_2\text{CuO}_{4+\delta}$: (a) at 4.7 T (\blacktriangle) and at 8.2 T (\circ) for sample A; (b) at 8.2 T for sample B. The dashed lines represent the Korringa behavior (see Table I) and the solid lines are the best fit for $T_1(T_c)/T_1(T) = \exp[-\Delta(T)/k_B T]$ with $\Delta(T)$ given by Eq. (3) and the parameters in Table II.

neon). This value of μ is too large and one can thus conclude a large degree of covalency must be involved in the Hg-O(2) bond. It is also possible there is a non-negligible contribution to $3K_{ax}$ from the spin susceptibility of the apical oxygen sites originating from the coupling with the holes associated with the excess interstitial oxygen.

The isotropic component of the shift tensor, K_{iso} , is difficult to estimate in absolute terms because of the possibility of moderate chemical shift values of the Hg^{2+} in the NMR reference aqueous solutions. For the reference used here, $\text{Hg}(\text{NO}_3)_2$, the effective gyromagnetic ratio $\gamma/2\pi$ is 7.6120 MHz/T. If one uses the value quoted⁹ for the bare nucleus, i.e., $\gamma/2\pi = 7.5901$ MHz/T then the values of K_{iso} in Table I should be increased by +0.33%. The decrease of K_{iso} below T_c is small (see Table I) and is of the same order of magnitude one expects from demagnetization effects.⁶ We conclude that accurate measurements of $K_{iso}(T)$, which can in principle give information about the Fermi liquid, appear problematic and should be attempted only if good single crystals of sufficient size become available.

Fortunately, the coupling of ^{199}Hg nuclei with the Fermi liquid of quasiparticles can be investigated through the spin-lattice relaxation rates, T_1^{-1} . The temperature dependence of $(T_1T)^{-1}$ is shown in Fig. 4 for both samples. The measurements were performed at the frequency in the spectrum (see Fig. 3) corresponding to the singularity (maximum amplitude) in the powder pattern due to the grains oriented perpendicular to the field. Thus the T_1^{-1} results refer approximately to the condition $\mathbf{H}_0 \perp c$ axis. Above T_c , a Korringa behavior of T_1^{-1} is observed with the values of $(T_1T)^{-1}$ reported in Table I. By using K_{iso} from Table I the experimental Korringa ratio $K_{iso}^2 T_1 T = 1.3 \times 10^{-5}$ (sec K) is close to

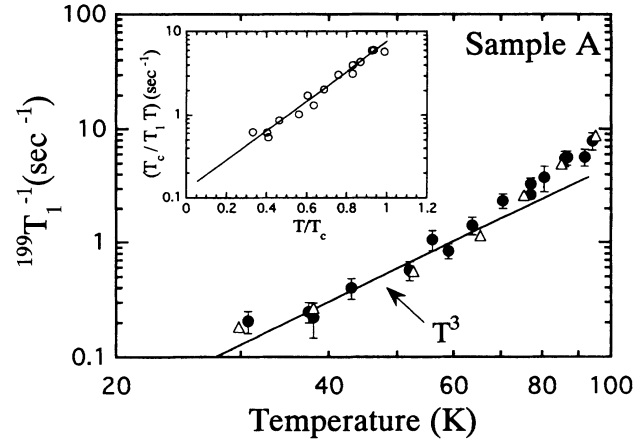


FIG. 5. Log-log plots of $^{199}\text{Hg } T_1^{-1}$ vs temperature for sample A which shows T^3 dependence at low temperatures: (Δ) at 4.7 T and (\bullet) at 8.2 T. The inset is a semi-log plot of (T_c/T_1T) data at 8.2 T vs (T/T_c) : It displays the fit according to Eq. (2) in the text with constants $P = 0.127$ Hz and $Q = 4.1$.

the theoretical value^{5,9} for a simple s -band metal, i.e., $(8\pi^2 k_B/h)(\gamma_N/\gamma_e)^2 = 0.83 \times 10^{-5}$ (sec K). No particular significance can be attached to this agreement because the exact value of K_{iso} depends on the NMR reference solution or $\gamma/2\pi$ value used. However, the Korringa behavior even for the underdoped sample B tells us that the effect of the antiferromagnetic (AF) fluctuations of Cu moments is small or is canceled exactly on Hg sites. The cancellation occurs only if the antiferromagnetic fluctuations are correlated in three dimensions. Both the values of the K_{iso} and $(T_1T)^{-1}$ are much smaller than in liquid Hg metal with a similar situation for the ^{89}Y NMR shift and relaxation rate in $\text{YBa}_2\text{Cu}_3\text{O}_7$ compared to Y metal. These observations are consistent with a low density of carriers in the CuO_2 planes and the position of the Hg (Y) ion out of the conducting planes.

As seen in Fig. 4 $(T_1T)^{-1}$ drops rather sharply below T_c indicating the opening of an energy gap. The quantitative interpretation of the temperature dependence of $(T_1T)^{-1}$ below T_c is complicated by the possible contribution to nuclear relaxation coming from the vortex lattice. The contribution can originate either from modulation of the internal field due to vortex thermal fluctuations or from relaxation in the normal metal at the core of the vortex and subsequently with spin diffusion to the nuclei in the superconducting regions.¹⁰ Both the above contributions depend on the applied field and can, in principle, be separated by looking at the limit of T_1^{-1} for $H_0 \rightarrow 0$.¹¹ As can be seen in Figs. 4 and 5, no detectable field dependence can be observed in the range 4.7–8.2 T for $\mathbf{H}_0 \perp c$ axis. Although a more complete study in oriented powders or single crystal is necessary to reach a firm conclusion, we are encouraged to analyze the data in terms of a dominant contribution to relaxation due to the coupling of Hg with the Fermi liquid of carriers.

As shown in the inset in Fig. 5, the data fit the behavior

$$T_c/T_1T = P \exp(QT/T_c), \quad (2)$$

which seems to be a general signature of the character of the superconducting state. The fit of Eq. (2) with different values

TABLE II. Optimum fitting parameters of the BCS theory to measured T_1^{-1} values.

	Sample A	Sample B	BCS (theory)
$\Delta(0)/k_B T_c$	1.61	0.94	1.76
$\Delta C/C$	0.91	0.87	1.41

of constant P and Q is found to hold in most Cu-based high- T_c superconductors and for the different nuclei probes.¹² However, no physical explanation for this behavior has been proposed.

A fit which bears physical meaning is the exponential fit: $T_1(T_c)/T_1(T) = \exp[-\Delta(T)/k_B T]$ which describes the decrease of quasiparticles available to relax the nuclei due to the opening of an energy gap $\Delta(T)$. The exponential decrease of T_1^{-1} should occur only for $T \ll T_c$ while near T_c one may have an enhancement due to the singular behavior of the density of states near the gap edges.¹³ This so-called Hebel-Slichter peak has not been reported in high- T_c materials and its absence has received many explanations, the most relevant being the anisotropy of the gap. As shown in Fig. 4 the data below T_c can be fit reasonably well with an exponential behavior and using a common interpolation formula for the temperature dependence of the gap:⁶

$$\Delta(T) = \Delta(0) \tanh \left[\frac{\pi k_B T_c}{\Delta(0)} \left(\frac{\Delta C}{C} \right)^{1/2} \left(\frac{T_c}{T} - 1 \right)^{1/2} \right], \quad (3)$$

where $\Delta C/C$ is the jump in specific heat at T_c . The parameters obtained from the fit are shown in Table II. The fit is good for sample A. However, for sample B there is a reduction of the quantity $(T_1 T)^{-1}$ starting at a temperature ~ 10 K above T_c . A similar effect was first observed for ^{63}Cu relaxation in $\text{YBa}_2\text{Cu}_3\text{O}_{6.63}$ (Ref. 14) and later recognized to be a common feature of oxygen-underdoped Cu-oxide high- T_c superconductors.¹⁵ The behavior is associated with the effect on AF fluctuations of the coupling of Cu moments

with the Fermi liquid, similarly to what was observed in heavy fermion systems.^{16,17} However, in the case of $\text{HgBa}_2\text{CuO}_{4+\delta}$, the coupling of ^{199}Hg to the Cu moments should be small judging from the Korringa behavior observed in the normal state, thus one should also consider alternative explanations such as a nonuniform distribution of the excess oxygen and the consequent distribution of T_c values. If the gap is anisotropic with a line of zeros on the Fermi surface, one should observe a T^3 temperature dependence of T_1^{-1} at $T \ll T_c$ in analogy to heavy-fermion systems.¹⁸ Martindale *et al.*¹¹ have recently fit the low-field relaxation rates of ^{63}Cu and ^{17}O in $\text{YBa}_2\text{Cu}_3\text{O}_7$ with a T^3 dependence claiming that the temperature dependence for $T \ll T_c$ was an indication of d -wave orbital pairing. A T^3 dependence was compared with our experimental data in Fig. 5. At $T \ll T_c$ the T^3 dependence may indeed be a better fit of the data. However, it is clear that a firm conclusion about the T dependence that fits the data best cannot yet be drawn.

In summary we have characterized the ^{199}Hg NMR in the newly discovered superconductor $\text{HgBa}_2\text{CuO}_{4+\delta}$. The main features are the very large anisotropic shift which is related to the linear Hg-O(2) bonding configuration and the Korringa-like temperature dependence of T_1^{-1} for $T > T_c$ and nearly exponential reduction of T_1^{-1} below T_c . Both these features indicate ^{199}Hg in Hg-based high- T_c superconductors is a good probe to test the opening of the superconducting energy gap in the quasiparticle spectrum. In order to obtain detailed information about issues such as the anisotropy of the gap and/or s -wave states vs d -wave states one must make more extensive measurements with an oriented powder or a single crystal which should include the field dependence for different orientations of the crystal.

The Ames Laboratory is operated for the U.S. Department of Energy by Iowa State University under Contract No. W-7405-Eng-82. This work was supported by the Director of Energy Research, Office of Basic Energy Sciences.

¹S. N. Pulinin *et al.*, Nature **362**, 226 (1993).

²J. L. Wagner *et al.*, Physica C **210**, 447 (1993).

³A. Tokiwa-Yamamoto *et al.*, Physica C **216**, 250 (1993).

⁴A. Schilling *et al.*, Physica C **216**, 6 (1993); U. Welp *et al.*, Appl. Phys. Lett. **63**, 693 (1993).

⁵A. Abragam, *The Principles of Nuclear Magnetism* (Clarendon, Oxford, 1961).

⁶M. Lee *et al.*, Phys. Rev. B **40**, 817 (1989).

⁷H. Alloul *et al.*, Phys. Rev. Lett. **70**, 1171 (1993).

⁸C. P. Slichter, *Principles of Magnetic Resonance*, 3rd ed. (Springer-Verlag, Berlin, 1990), p. 108.

⁹G. C. Carter, L. H. Bennett, and D. J. Kahan, *Metallic Shifts in*

NMR (Pergamon, New York, 1977), Pt. I.

¹⁰F. Borsa *et al.*, Phys. Rev. Lett. **68**, 698 (1992); J. A. Martindale *et al.*, *ibid.* **68**, 702 (1992).

¹¹J. A. Martindale *et al.*, Phys. Rev. B **47**, 9155 (1993).

¹²S. E. Barrett *et al.*, Phys. Rev. Lett. **66**, 108 (1991).

¹³L. C. Hebel and C. P. Slichter, Phys. Rev. **113**, 1504 (1959).

¹⁴W. W. Warren, Jr. *et al.*, Phys. Rev. Lett. **62**, 1193 (1989).

¹⁵M. Horvatic *et al.*, Phys. Rev. B **47**, 3461 (1993).

¹⁶F. Borsa *et al.*, Appl. Magn. Reson. **3**, 509 (1992).

¹⁷K. Levin *et al.*, Physica C **175**, 449 (1991); J. P. Lu *et al.*, *ibid.* **179**, 191 (1991).

¹⁸M. Kyogaku *et al.*, J. Phys. Soc. Jpn. **62**, 4016 (1993).